

ASSESSMENT OF LNG BUNKERING ACCIDENTS

Peter Vidmar, Andrej Androjna

University of Ljubljana (Slovenia)

Abstract. The maritime safety is of great concern for the entire maritime community. Ships using LNG for propulsion are already sailing the seas, but the majority of the ports are not yet prepared for this kind of supply. As the process of LNG bunkering is only seemingly similar to traditional oil bunkering or liquid loading, dealing with the technical and safety challenges is much more subject of investigation. In this paper, the dispersion part of the consequences of LNG release, pooling, evaporation and dispersion during the future bunkering operation in the port of Koper, Slovenia, where the populated area (city) is located in close proximity are examined. We follow the comparison of three different tools, namely the Unified Dispersion Model (UDM) implemented by the software PHAST from DNV-GL® and two CFD (FDS - Fire Dynamics Simulator from NIST and Ansys Fluent®) in the same case scenario. Geometry, initial and boundary conditions are assumed to be the same as far as possible, according to the limitations of the respective software tools.

Keywords: LNG; bunkering; risk assessment; dispersion; CFD; UDM model

Introduction

Pollution prevention in the maritime industry¹⁾ has led to significant interest in the use of Liquefied Natural Gas (LNG) as an alternative clean maritime fuel instead of fuel oil. However, conversion to LNG fuel is a lengthy process that faces many obstacles, such as major technical differences in engines, logistics, and supply infrastructure. LNG is a cryogenic liquid produced by cooling natural gas to about -163 °C (110 K) to reduce its volume by a factor of about 600. While the safety of large LNG carriers and their associated regasification terminals has been the subject of much study in the past, the coming widespread use of LNG as a fuel will require the design of marine bunkering operations, usually in or around port areas. This brings a new dimension to the safety of ship operations in ports and has been the subject of extensive literature reviews (Aneziris 2020). Several standards, guidelines and regulations related to LNG fuel technology are rapidly becoming available to cover the technical and organizational requirements. In addition, the limited amount of research on risk assessment indicates that there are still many unanswered questions due to the specific properties of LNG, e.g.: Vapours have an

initial negative buoyancy, the evaporation rate during spills is still uncertain, or the vapour can sustain rapid phase transition phenomena (RPT). In addition, the effects of light hydrocarbons in LNG composition affect flammability limits and other properties (Sandia 2014; Cleaver et al. 2007; Pio et al. 2018).

The purpose of this paper is to address three of the above issues. First, a review of the available studies that report on the methods and tools used to evaluate the evaporation rate from a pool formed over water (sea). Indeed, the work and experimental data suggest that the formation of the LNG pool over deep water is a complex process and that its modelling and the consideration of the total evaporation flux (starting point for the dispersion of the flammable gas) deserves special attention (Fay 2007; Horvat 2018). Two, port-specific safety studies²⁾ (Rambøll 2013) commonly use integral dispersion models such as the Unified Dispersion Model (UDM) implemented in the PHAST software^{3),4)}. These models cannot account for complex terrain geometries and spatial obstacles in the model domain, as mentioned in the points above. To this end, many papers and some case studies also use some of the available CFD modelling tools that can adequately account for complex geometry in a 3D model of the case (Hansen et al. 2009; Jeong et al. 2017; Jeong et al. 2018; Horvat 2018; Park et al. 2018; Rambøll 2013; Scandpower 2012).

In this regard, the paper will explore these issues in the context of realistic ship-to-ship (STS) bunkering operations between a bunkering vessel and a large container ship. In particular, we will examine the available information on the LNG evaporation rate from the pools formed above the sea surface, the available UDM dispersion model through the PHAST tool^{3),4)} and two CFD dispersion modelling tools, namely the Fire Dynamics Simulator (FDS) from National Institute of Standard and Technology (NIST) of the USA (McGrattan et al. 2018) and the Ansys Fluent⁵⁾, as well as the effect of bunkering micro-locations and local meteorological conditions on the dispersion into the ambient air. To our knowledge, such comparative modelling of potential LNG evaporation and dispersion has not yet been reported in the context of assessing safe distances for bunkering operations.

The knowledge about the consequences of a LNG dispersion could lead to the understanding of how to plan the safety management in a port as well as in the neighbour populated area.

Methods, tools and data used

Evaporation rate from pools over deep water

Few data for small-scale LNG releases – which may be considered typical for STS operations – are available in the literature. According to (Luketa-Hanlin 2006), the mass evaporation rate m''_{ev} can vary between 0.029 to 0.185 kg s⁻¹ m⁻² as a mean value. This range of values could be considered for CFD or other purposes, in the absence of more accurate values. Quite clearly, uncertainties arise from pool dimension

(effect of Reynolds number), pool formation (discharge rate) and atmospheric conditions. The given range is however confirmed by several experimental tests. On average, the pool is considered at 112 K, the atmospheric and water (when applicable) temperatures are 298 K and 293 K, respectively. The experimental tests of the Bureau of Mines, as reported by (Burgess et al. 1972) have evaluated a value of $0.181 \text{ kg s}^{-1} \text{ m}^{-2}$ and $0.155 \text{ kg s}^{-1} \text{ m}^{-2}$. Sandia (2004) measured a value of $0.195 \text{ kg s}^{-1} \text{ m}^{-2}$. On the contrary, (Luketa-Hanlin 2006), in the well-known test of Maplin Sands measured $0.085 \text{ kg s}^{-1} \text{ m}^{-2}$ (possibly due to the large pool scale and the inverse relation with the pool radius). Most of the simplified studies have adopted $0.181 \text{ kg s}^{-1} \text{ m}^{-2}$ as a reference value, following a conservative approach. However, similar evaporation rates have been largely associated with the case of LNG pool fire as well (Fay 2006). Hence, the implementation of similar values for dispersion/potential flash fire scenario implies an arguable assumption of the negligible effect of heat generated by the flame above the pool on the evaporation. In this view, the adoption of a more fundamental-based approach is desirable. Among the others, Klimenko's model (Klimenko 1981) estimates the heat transfer coefficient based on Nusselt, Prandtl, and Archimedes numbers in case of liquid evaporation on a calm liquid surface. The presence of the latter dimensionless number suggests the significance of the effect of a dense cloud of fuel vapours in the proximity of the pool on the evaporation rate. (Conrado et al. 2000) have validated the abovementioned model for the LNG case, as well, obtaining an evaporation rate of $0.072 \text{ kg s}^{-1} \text{ m}^{-2}$. Eventually, the effect of water turbulence can be assessed separately. Indeed, an experimental campaign on lab-scale facilities conducted by (Morse et al. 2011) have observed an almost linear trend for the water surface turbulence intensity for LNG evaporation rate. Experimental contingencies (i.e., ice formation) have limited the analysis to velocity fluctuation smaller than 0.1 m s^{-1} , in agreement with theoretical treatment reported by (Vesovic 2007) supposing an abrupt decrease in the surface temperature of water and ice formation in the case of confined and shallow-water surfaces. Nevertheless, in the first approximation, an extrapolated value has been reported for the case of null velocity fluctuation, assuming a linear trend (i.e., $0.053 \text{ kg s}^{-1} \text{ m}^{-2}$). The reported value results in substantial agreement with the theoretical-based estimation reported by Conrado and Vesovic. Eventually, we will consider two values: the conventional at $0.181 \text{ kg s}^{-1} \text{ m}^{-2}$, and the alternative at $0.053 \text{ kg s}^{-1} \text{ m}^{-2}$.

UDM dispersion model & tool used

Standard off-the-shelf methods and tools are widely used to model the consequences of the releases of hazardous materials. In that respect, we used an integrated software package DNV GL PHAST version 8.22³⁾. The programme tool already contains a database with the properties of pure substances. The programme uses the Unified Dispersion Model (UDM) to model jets, dense, buoyant and

passive dispersion including droplet rainout and re-evaporation (DNV GL 2017a). The model allows for continuous, instantaneous, constant finite-duration, and general time-varying releases; nevertheless, time-varying releases are treated as a series of a maximum of 10 pseudo-steady-state steps, thus providing only a rough representation of the trend over time of the release characteristics.

The modelling was limited to the use of the user-defined release case, prescribing the LNG release rate & duration at the set process and case conditions (later reported in Table 1.), resulting in data on the LNG pool formation and downwind distances to UFL, LFL and LFL/2 concentrations in ambient air (16.5 %, 5 % and 2.5 % vol., respectively).

Related to the topic of this paper it is worth to note that the built-in modelling considers the conventional LNG evaporation rate from a pool on the water at $0.18 \text{ kg s}^{-1} \text{ m}^{-2}$ ⁶, adopted from (Burgess et al. 1972).

CFD dispersion modelling using FDS tool

A simplified 3D layout, representative of the bunkering terminal and nearby city, was implemented in FDS for the characterization of accidental release of LNG on water, by using the user-friendly interface PyroSim (McGrattan et al. 2020). The time-depending properties were visualized using the SmokeView tool (SMV). FDS is an open-source software developed by the National Institute of Standards and Technology (NIST) suitable for the modelling of low Mach problems. It is based on the Large Eddy Simulation (LES) approach as a low-pass filter for Navier-Stokes equations and it has been extensively validated for accidental release of LNG (Sagaut et al. 2002; Zhang et al. 2016; Pio et al. 2019; Zheng et al. 2019).

Scenario modelling

The gas dispersion caused by LNG leaks during bunkering accident was simulated with the Fire Dynamics Simulator (FDS) (McGrattan et al. 2018). The gas dispersion is simulated using LES in FDS where Favre filtering is used in the momentum equation, mass, energy, and species combined with state equations for ideal gases. In the present study, the source term m_{α}'' , the mass flux of the methane species is added to the species transport equations and is defined on the boundary of the modelled LNG pool. The simulation of combustion is avoided in this study as the main interest is to find the area that could be affected by the concentration of the methane gas.

The 3D domain size is $1115 \times 953 \times 83$ m and was discretized with finite volume meshes having a resolution of $2 \times 2 \times 0.7$ m. The space discretization of the mass equations, motive quantity and heat energy is derived with the method of finite difference in the central differential scheme in a square net. The time discretization of the transfer equations is made on an explicit scheme of predictor-corrector.

After the grid independence analysis for gas dispersion, a total of 24,000,000 cells was used, and the cell aspect ratio was set to $3 \times 3 \times 1$ in the Cartesian coordinate system. In x and y directions the size of the cell is not optimal but fits the simulation convergence criteria.

The transient calculation is set to 400 seconds, as the results showed later the LFL/2 concentration is not any more present after that time (in fourth micro-simulation reported in coming section this was doubled). The main points of the observations are the methane concentration distributions at 5 and 2.5 % by volume, corresponding to the LFL and LFL/2 concentrations, respectively.

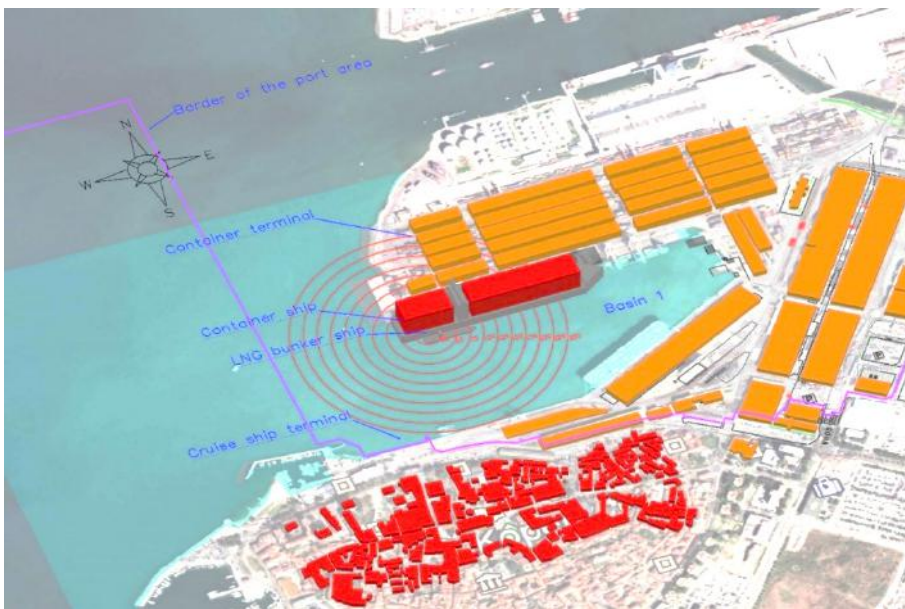


Figure 1. Area and geometry of the model

Case study

The port of Koper is a multi-purpose port located in the north Adriatic Sea. Located directly in contact with the old town centre, it is always subjected to safety assessments, as the port activities have potential risks to the neighbouring population. The strategy of the port is also to provide, in the near future, the possibility of LNG bunkering for all or at least some types of ships. Potentially, the most promising are container ships and cruise ships. Terminals for both types of ships are located in basin 1, on the north side (berth 7) serving the container ships and the passenger terminal on the south (berth 1) serving cruise ships. The closest populated area is about 50 meters south of berth 1. The houses in the old town are

about 10 m above sea level. The case study assumes the two most probable positions of receiving and bunkering ships, namely, berth 1 and berth 7. The receiving ships are assumed to be large: the container ship is a size of a triple E (length of 400 m) and a passenger cruise ship length is about 350 m. The height of the receiving ships is also important, because compared to the size of a bunkering ship; they represent a wind barrier that can keep them in a leeward from the wind. The situation and 3D model are presented in Figure 1.

Meteorological situation

The relevant meteorological data for the Port of Koper were obtained from the port's automatic meteorological stations. The wind rose profile for the year 2020 is presented on Figure 2. It can be concluded that the dominant wind speed is at about 2 m/s, the prevalent wind direction is from the east-south-east (direction at about 110°), followed by west-north-west direction (direction at about 300°).

Accordingly, the wind speed was set to 2 m/s at the height of 10 m above the sea and the atmospheric boundary layer is assumed using Monin-Obukhov similarity theory (McGrattan et al. 2018). Both mentioned wind directions were further considered in the modelling.

The initial temperature of the atmosphere was set to 20 °C at 50 % relative humidity. The boundary land surface was created under adiabatic conditions, and the other boundary conditions were set as open to simulate general inflow and outflow conditions. The sea surface is applying the water thermal properties to simulate the heat transfer between cold natural gas and sea surface.

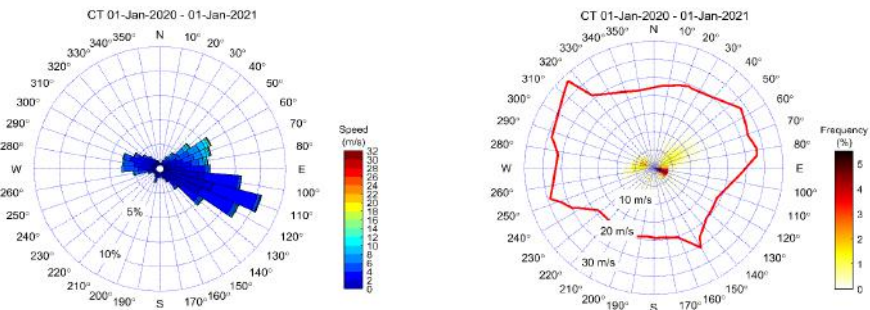


Figure 2. Wind rose for the container terminal and the cruise ship terminal

Release scenario

The technologies usually consider operations with LNG stored at about -164 °C (109 K) and 6 bar pressure difference at the ship-to-ship bunkering interface (Rambøll 2013; Scandpower 2012). The hoses used are DN150 size and a typical

flow rate considered is $350 \text{ m}^3 \text{ h}^{-1}$ delivered by the submerged centrifugal pumps. In the case of the hose rupture, the release from the liquid phase branch is the most important and due to the pumps impeller, the flow rate can increase due to the pressure drop maximum by a factor of 1.2 to 1.5 (Rambøll 2013). In this paper, we consider a factor of 1.3. Considering the LNG density of 420 kg m^{-3} this brings to the expected release rate of about 53.2 kg s^{-1} . On the other hand, there are many safety systems planned to stop small and large leaks, including the presence of the operators. As a rather conservative estimation, we consider that the rupture is stopped within 120 s from the start.

The most important input parameters used in modelling by all three tools are summarized in Table 1.

Table 1. Summary of important modelling parameters of the release scenario.

Parameter	Unit	Value
Source term data		
Model substance released	-	methane
Temperature	°C	-164
Pressure difference at the release point (head)	bar	6
Hose diameter	mm	150
Release rate	kg s^{-1}	53.2
Release duration	s	120
Meteorological situation		
Wind speed	m s^{-1}	2
Wind stability category (PG)	-	D
Wind direction(s)	°	east-south-east (110°); west-north-west (300°)
Air temperature	°C	25
Location data		
Substrate type	-	deep water ^a
Bund presence	-	none
Substrate temperature	°C	20
Substrate surface roughness parameter (z_0)	m	0.005

Notes: ^a – a channel with open both ends is formed between both ships (UDM model).

Following the spill of LNG over the sea surface, transient evaporation and boiling of the natural gas starts. However, the remaining LNG spreads over the sea surface as a pool. The modelling of the pool formation and natural gas evaporation into the dispersion modelling is integrally done within the DNV GL PHAST tool. Results obtained in the coming section suggest that the pool reaches the maximum size at 120 s and the largest area of about 300 m^2 considering conventional pool evaporation

rate of $0.18 \text{ kg s}^{-1} \text{ m}^{-2}$. In FDS model, we considered the LNG pool formation data as presented in Figure 3 due to the necessary modelling simplifications in the pool area evaporation.

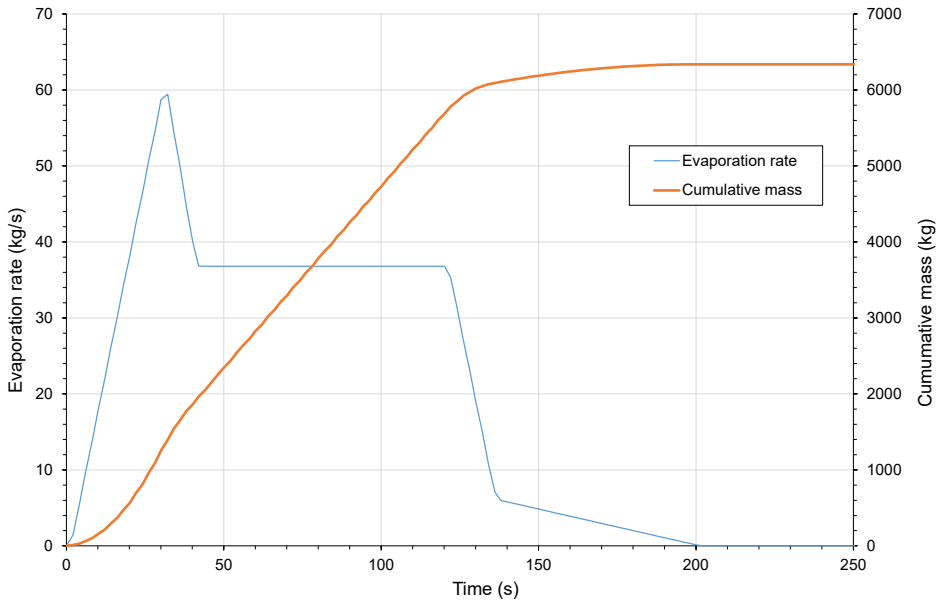


Figure 3. LNG evaporation

Results and discussion

Results considering the Port of Koper real terrain

The configuration of the berths and moored ships are pre-determined by port. Geometrically, most of the influence on the fluid dynamics around the ship comes from the ship type and its particular freeboard. The large freeboard represents a barrier to a downwind flow and a significant source of vortices on a leeward side. This is mostly the case of a container ship exposed to north or north-west wind. A series of three micro-simulation results are presented considering the conventional LNG evaporation rate of $0.181 \text{ kg s}^{-1} \text{ m}^{-2}$. The first is when the container ship is moored at berth 7 at the north side of basin 1 and the wind direction is from 300° . The second and the third micro-simulations locate the cruise ship at the south side of basin 1 at berth 1 and the wind directions are from 300° and 110° , respectively.

The first micro-simulation is presented as a set of methane concentration snapshots in time obtained by the FDS model in Figure 4. The figures present the top view of the cloud; however, the longitudinal cross section is presented separately

to indicate the influence of the ship hull to the cloud movement. The presence of the ship importantly influences the dispersion of the gas cloud, its shape and length. The figure shows the LFL cloud concentration at different time steps, but the shape of the cloud is not even directed downwind but dilutes due to the vorticity before reaching the mainstream of the wind.

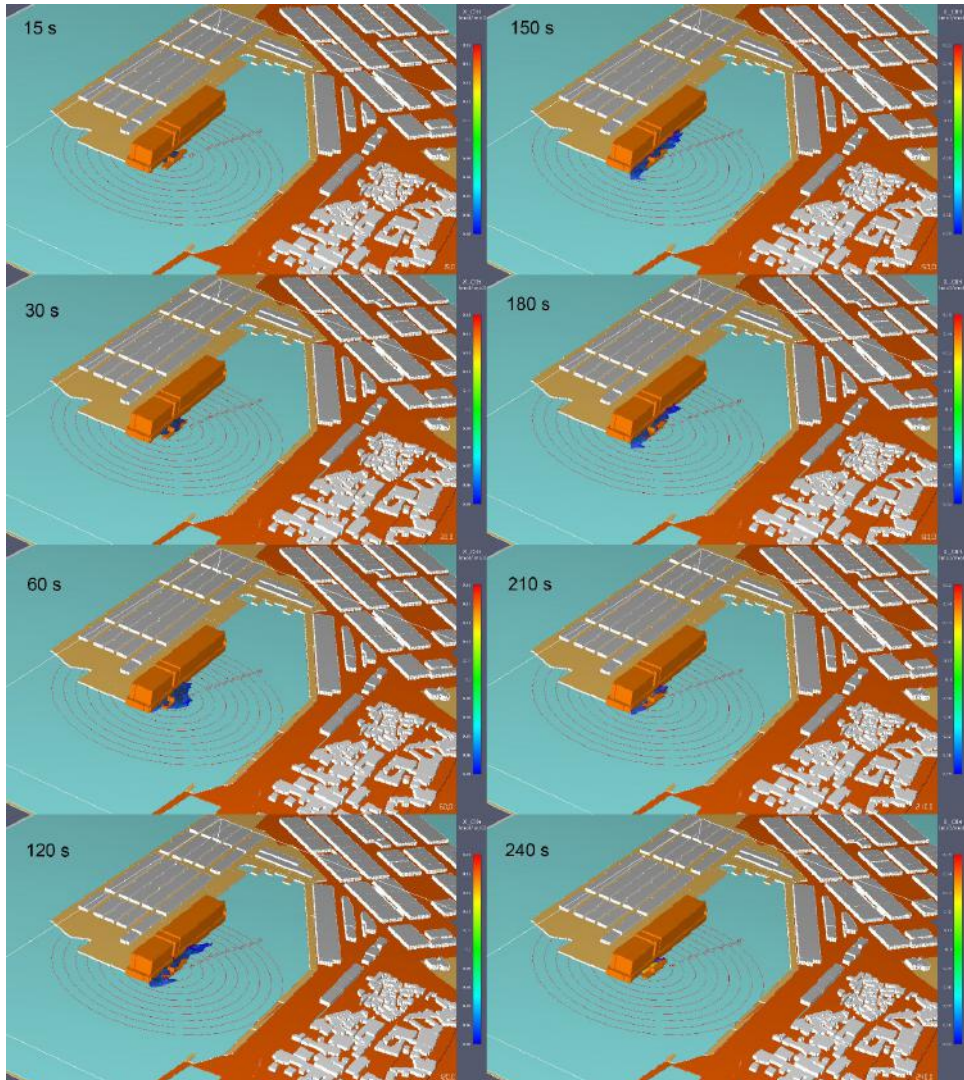


Figure 4. Isosurface for North wind model

The comparison of downwind distance and cloud area to LFL concentration vs time for FDS and Fluent models for this micro-simulation is presented in Figure 5. We can observe that both models agree very well related to the downwind distance vs. time profiles, however, Fluent reports much lower cloud area figures. We can also observe that the maximum cloud distance is about up to 30 % lower in comparison to the case of considering flat terrain (previous section).

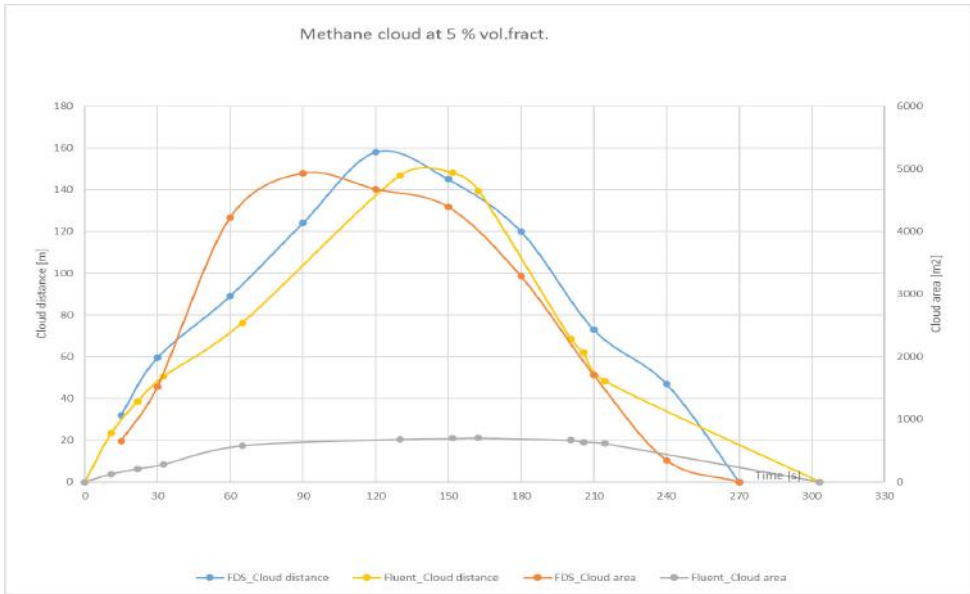


Figure 5. LNG cloud dispersion results

The second micro-simulation is presented as a set of methane concentration snapshots in time obtained by the FDS model in Figure 6. The dispersion of gas cloud concentration is observed for the LFL concentration. The cloud is directed downwind along the shipside and reaches a distance of about 400 m from the pool. In this case, the cloud does not reach the shore area but remains and dilutes on a seaside. The comparison of downwind distance and cloud area to LFL concentration vs time for FDS and Fluent models for this micro-simulation is presented in Figure 7. The velocity of the cloud spread is near-constant along its path (FDS model). The area that the gas cloud covers is at most about 16000 m², which is more than three times larger than in the first micro-simulation, but close to the area from the case considering flat terrain (previous section). The reason is the dispersion of the gas is less influenced by environmental geometry. The ship's position alongside the direction of the wind acts as a duct or channel and is not a source of larger vortices that would contribute to faster dispersion of the gas.

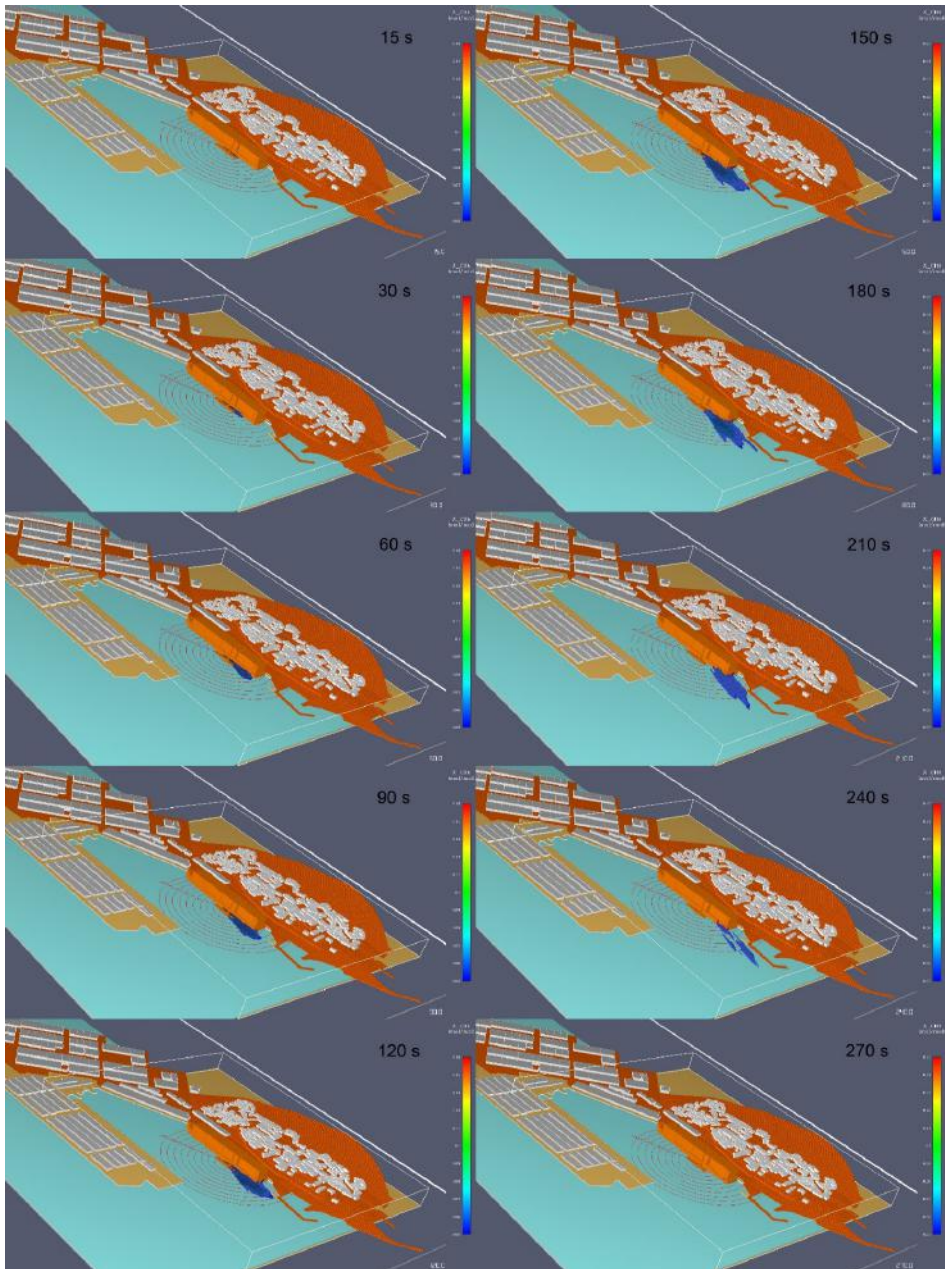


Figure 6. Isosurface for East wind model for cruise ship

This influence is observed especially because the size of the ship is much larger than the bunkering ship and the pool size, and geometrically covers most of the observed gas cloud. On the other hand, estimations obtained by Fluent indicate a flammable region limited to the ship boundaries (i.e., to the duct formed by the obstacles). The comparison of the area and size in the downwind direction suggests that a less effective dispersion can be assumed with respect to the other models employed in this work since only the direction driven by wind is characterized by similar results. Considering that the reported results refer to a given distance from the sea level, this discrepancy can be attributed either to the different estimation of fuel density with cryogenic temperature leading to higher cloud or larger average concentration of the fuel within the cloud.

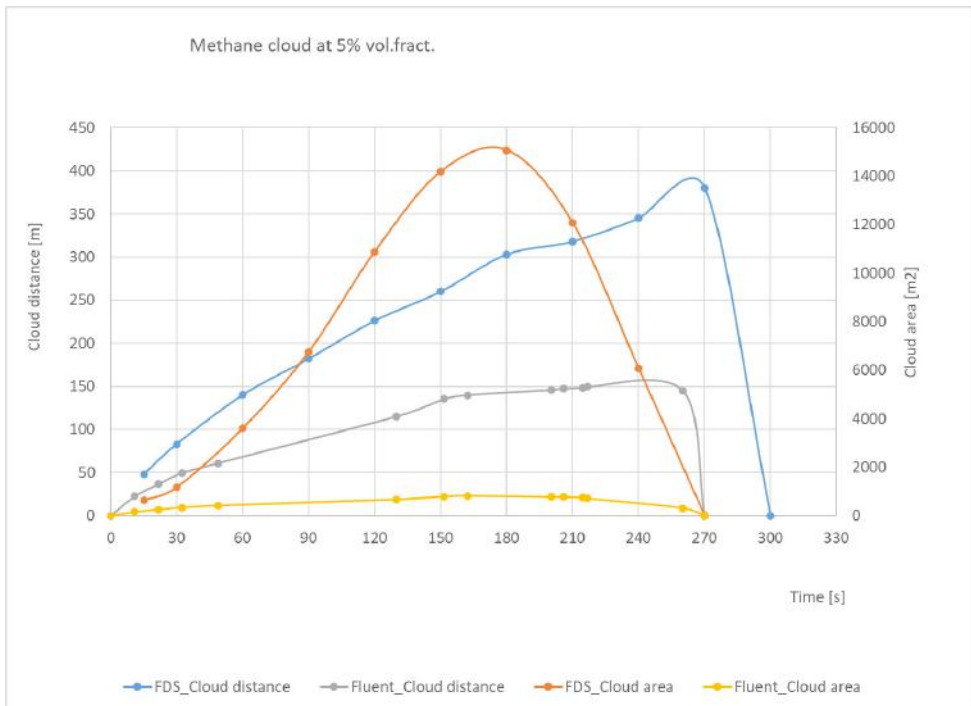


Figure 7. LNG cloud dispersion results

The third micro-simulation is presented as a set of methane concentration snapshots in time obtained by the FDS model in Figure 8. The dispersion of gas cloud concentration is observed for the LFL concentration. It can be observed that even if the wind is oriented towards the city the size of the container ship acts as a barrier and redirects the airflow along the seaside of the hull to the direction of the

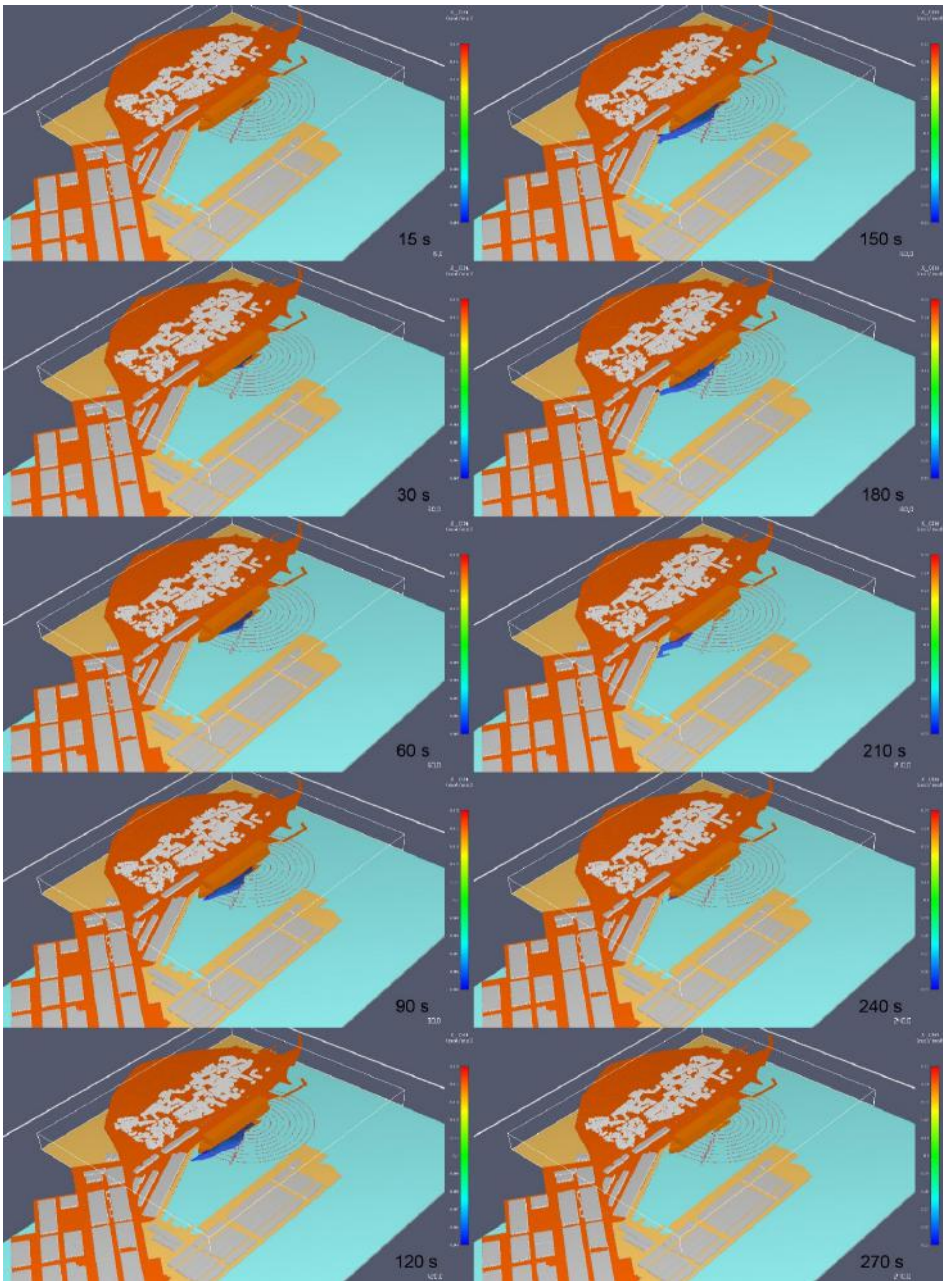


Figure 8. Isosurface for North wind model for cruise ship

general cargo terminal (east). In any case, the gas cloud stays during the simulation within the port area limits.

The comparison of downwind distance and cloud area to LFL concentration vs time for FDS and Fluent models for this micro-simulation is presented in Figure 9. Data resulting from the LES simulations (i.e., FDS) indicate almost double downwind distances than the RANS case (i.e., Fluent), confirming the relevance of turbulence modelling for the evaluation of dispersion scenarios. Indeed, less accurate grids for turbulence imply less effective mixing, leading to a higher concentration of fuel within the cloud, thus smaller flammable areas. The analysis of the cloud distances and area vs. time shows that the gas cloud reaches a distance of about 370 m and then disappears. The distance is similar to the second micro-simulation, even though the maximum area of the cloud is about 25 % smaller. The gas cloud is again canalised by the ship hull and is less perturbed, keeping the slender shape along the hull. The influence of the vorticity caused by faster gas dispersion is not visible and can be observed from the distribution of the cloud area during the simulation. The velocity of the cloud spread (distance, area) is near-constant along its path till the stop of the release at 120 s (FDS model). This indicates the cloud is not perturbed significantly during its dispersion.

Similar trends describing the evolution of the cloud along with the time were reported for the investigated scenarios, suggesting a limited impact due to the layout configuration.

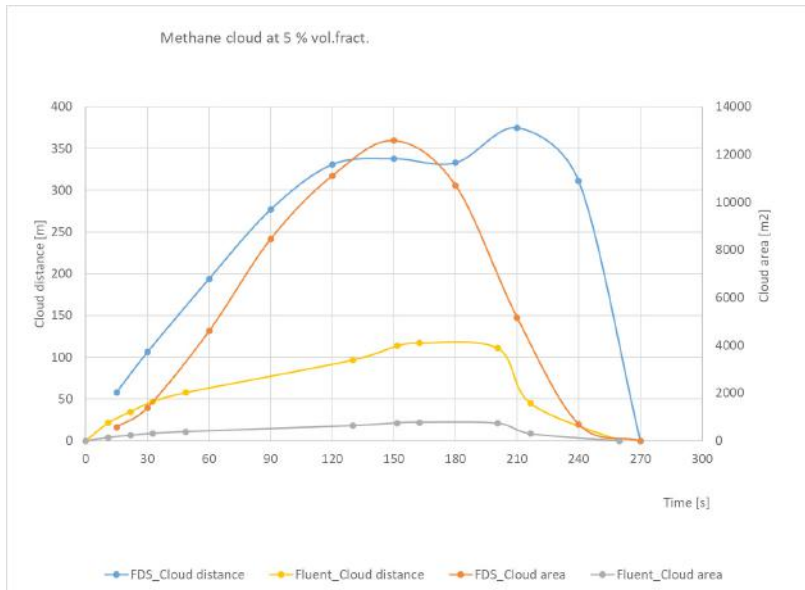


Figure 9. LNG cloud dispersion results

The comparison of the presented results from different scenarios indicates that either the extension of the flammable area or the maximum downwind distance having a flammable mixture are mainly affected by the congestion, with a limited impact on the considered evaporation rate. Regardless of the implemented sub-model and layout, the evolution of the cloud size to time can be represented by three stages: initial growth, pseudo-steady state, and decay. However, after an initial phase, the presence of obstacles decelerates the growth phase and reduces the duration of the pseudo-steady state stage. Considering that the evaporation rate is kept constant at this stage, these trends imply that a higher average concentration of methane is reached within the cloud. Hence, the occurrence of stratified mixtures can be hypothesized. Hence, the estimation of the standoff distances in case of accidental release of cryogenic liquids is strongly influenced by the selected height from the sea level. Besides, regular cloud edges may be inferred by the smoothness of the reported trends from results deriving from Ansys Fluent, only. Hence, this observation is affected by the sub-model considered for turbulence.

Conclusions

The simulations of LNG spill and gas dispersion presented in this paper are limited to the most credible scenario. The limits of the spill are based on guidelines and standards for marine equipment engineering and are assumed to apply to technical failures and marine accidents in ports. In these cases, LNG spill is predictable and controlled by the ship safety system including emergency shutdown of the bunkering process. The leakage time, spill quantity and pool area boundaries assumed in the model are derived from the assessed bunkering process and represent the boundaries for the safety assessment. According to these assumptions, the three case micro-simulations are verified using three different models, one UDM and two CFD. The results show that all three models give comparable results for the gas dispersion distance in flat terrain, although Fluent calculates a smaller area of the cloud in all three cases. The results of the analysis of the results show a significant influence of the geometry around the LNG pool, i.e. the large ship acts as a barrier increasing the vorticity when it is upwind of the pool and acts as a channel when it is downwind of the pool. The UDM model does not account for the heights of the geometry and is therefore not reliable for LNG spills where the vaporized gas cloud remains stratified a few meters above the ground and is also strongly influenced by lower structures such as piers, houses and moored ships. CFD should be considered for gas dispersion in these cases with a defined gas evaporation rate obtained from experimental tests or simulated separately and validated for a specific spill case.

NOTES

1. IMO (International Maritime Organisation), 1997. Resolution MEPC.75(40) Amendments to the Annex of the Protocol of 1978 relating to the International convention for the prevention of pollution from ships, 1973. London: IMO. www.imo.org.
2. DNV, 2012. Report Port toolkit risk profile LNG bunkering. Port of Rotterdam, Ministry of Infrastructure & Environment, Port of Antwerp, Port of Amsterdam and Zeeland Seaport. Report No./DNV Reg No.: PP035192-R2 Rev. 2, 28 August 2012. [<http://www.lngbunkering.org/lng/sites/default/files/2012%2C%20DNV%2C%20Port%20Toolkit%20Risk%20Profile%20LNG%20bunkering.pdf>]
3. DNV GL, 2017a. Report THEORY Unified Dispersion Model (for registered users).
4. DNV GL, 2020. More info on PHAST and SAFETI software packages [<https://www.dnvgl.com/services/qra-and-risk-analysis-software-phast-and-safeti-1676> (27.8.2020)]
5. Ansys Fluent, 2021. More info on Ansys Fluent Fluid Simulation Software at <https://www.ansys.com/products/fluids/ansys-fluent>
6. DNV GL, 2017b. Report THEORY Pool Vaporisation (for registered users).
ISO (International Organisation for Standardisation), 2015. ISO/TS 18683: Guidelines for systems and installations for supply of LNG as fuel to ships. Geneva: ISO. <https://www.iso.org/standard/63190.html>

REFERENCES

- Aneziris, O., Koromila, I., Nivolianitou, Z., 2020. A systematic literature review on LNG safety at ports. *Safety Science* **124**, 104595. Available from: <https://doi.org/10.1016/j.ssci.2019.104595>
- Burgess, D., Biordi, J., Murphy, J., 1972. Hazards of spillage of LNG into water. *NAT. TECH. INFO. SERV.* Available from: <https://apps.dtic.mil/sti/citations/AD0754498>
- Cleaver, P., Johnson, M., Hob, B., 2007. A summary of some experimental data on LNG safety. *Journal of Hazardous Materials* **140**, 429 – 438. Available from: <https://doi:10.1016/j.jhazmat.2006.10.047>
- Conrado, C., Vesovic, V., 2000. The influence of chemical composition on vaporisation of LNG and LPG on unconfined water surfaces. *Chem. Eng. Sci* **55**, 4549 – 4562. Available from: [https://doi.org/10.1016/S0009-2509\(00\)00110-X](https://doi.org/10.1016/S0009-2509(00)00110-X)
- Fay, J.A., 2006. Model of large pool fires. *Journal of Hazardous Materials* (136), 219 – 232. Available from: <https://doi.org/10.1016/j.jhazmat.2005.11.095>
- Fay, J.A., 2007. Spread of large LNG pools on the sea. *Journal of Hazardous Materials* (140), 541 – 551. Available from: [doi:10.1016/j.jhazmat.2006.10.024](https://doi.org/10.1016/j.jhazmat.2006.10.024)

- Hansen, O.R., Ichard, M., Davis, S.G., 2009. Validation of FLACS for vapor dispersion from LNG Spills: model evaluation protocol. In: *12th Annual Symposium*, 712 – 743. Mary Kay O'Connor Process Safety Center.
- Horvat A., 2018. CFD methodology for simulation of LNG spills and rapid phase transition (RPT). *Process Safety and Environmental Protection* **120**, 358 – 369. Available from: <https://doi.org/10.1016/j.psep.2018.09.025>
- Jeong, B., Lee, B.S., Zhou, P., Ha, S.-M., 2017. Evaluation of safety exclusion zone for LNG bunkering station on LNG-fuelled ships. *J. Mar. Eng. Technol.* **16**(3), 121 – 144. Available from: <https://doi.org/10.1080/20464177.2017.1295786>.
- Jeong, B., Lee, B.S., Zhou, P., Ha, S.-M., 2018. Determination of safety exclusion zone for LNG bunkering at fuel-supplying point. *Ocean Eng.* **152**, 113 – 129. Available from: <https://doi.org/10.1016/j.oceaneng.2018.01.066>
- Klimenko V. V., 1981. Film boiling on a horizontal plate - new correlation. *Int. J. Heat Mass Transf.* **24**, 69 – 79. Available from: [https://doi.org/10.1016/0017-9310\(81\)90094-6](https://doi.org/10.1016/0017-9310(81)90094-6)
- Luketa-Hanlin A., 2006. A review of large-scale LNG spills: Experiments and modeling. *Journal of Hazardous Materials* (132), 119 – 140. Available from: DOI: 10.1016/j.jhazmat.2005.10.008
- McGrattan, K., et al., 2018. *Fire Dynamics Simulator Technical Reference Guide*. Natl. Inst. Stand. Technol. Spec. Publ. 1018-1.
- McGrattan, K., et al., 2020. *PyroSim User Manual v. 2020-2*. Thunderhead Engineering.
- Morse, T. L., Kytömaa, H. K., 2011. The effect of turbulence on the rate of evaporation of LNG on water. *J. Loss Prev. Process Ind.* **24**, 791 – 797. Available from: <https://doi.org/10.1016/j.jlp.2011.06.004>
- Park, S., Jeong, B., Young Yoon, J., Paik, J.K., 2018. A study on factors affecting the safety zone in ship-to-ship LNG bunkering. *Ships and Offshore Structures.* **13**(sup1), 312 – 321. Available from: DOI: 10.1080/17445302.2018.1461055
- Pio, G., Carboni, M., Iannaccone, T., Cozzani, V., Salzano, E., 2019. Numerical simulation of small-scale pool fires of LNG. *Journal of Loss Prevention in the Process Industries* **61**, 82 – 88.
- Pio, G., Salzano, E., 2018. Laminar Burning Velocity of Methane, Hydrogen, and Their Mixtures at Extremely Low Temperature Conditions. *Energy & Fuels* **32**, 8830 – 8836.
- Pio, G., Salzano, E., 2018. Flammability parameters of liquefied natural gas. *Journal of Loss Prevention in the Process Industries* **56**, 424 – 429. Available from: <https://doi.org/10.1016/j.jlp.2018.10.002>

- Rambøll, 2013. *Risk analysis LNG bunkering of vessels with passengers on board*. Client: DSB, report type joint report, 21/08/2013. Available from: <https://www.sdir.no/en/shipping/accidents-and-safety/safety-investigations-and-reports/risk-analysis-of-lng-bunkering/>
- Sagaut, P., 2002. *Large Eddy Simulation for Incompressible Flows, second edition*. Berlin Heidelberg: Springer-Verlag. ISBN 978-3-662-04697-5.
- Sandia, 2014. Guidance on Risk Analysis and Safety Implications of a Large Liquefied Natural Gas (LNG) Spill Over Water. *Report SAND2004-6258*. Available from: <https://www.nrc.gov/docs/ML0933/ML093350855.pdf>
- Scandpower, 2012. Comparative study on gas dispersion. *Report no. 101368/R1* [24 January, 2012], Client DSB. Available from: <https://www.dsb.no/globalassets/dokumenter/rapporter/andre-rapporter/final-report-scandpower-2012.pdf>
- Vesovic, V., 2007. The influence of ice formation on vaporization of LNG on water surfaces. *J. Hazard. Mater.* **140**, 518 – 526. Available from: DOI: 10.1016/S0009-2509(00)00110-X
- Zhang, Q., Liang, D., 2016. Numerical simulations of LNG vapor dispersion from LNG jetting in different directions. *Procedia Engineering* **135**, 316 – 321. Available from: <https://doi.org/10.1016/j.proeng.2016.01.136>
- Zheng, J., Chen, L., Wang, J., Zhou, Y., Wang, J., 2019. Thermodynamic modelling and optimization of self-evaporation vapor cooled shield for liquid hydrogen storage tank. *Energy Conversion and Management* **184**, 74 – 82.

✉ **Peter Vidmar**

Faculty of Maritime Studies and Transport
University of Ljubljana
Ljubljana, Slovenia
E-mail: Peter.Vidmar@fpp.uni-lj.si

✉ **Andrej Androjna**

ORCID iD: 0000-0002-5105-9884
Faculty of Maritime Studies and Transport
University of Ljubljana
Ljubljana, Slovenia
E-mail: Andrej.Androjna@fpp.uni-lj.si